Comptes Rendus
Géoscience — Sciences de la Planète
2021, 353, nº S2, p. 273-288
https://doi.org/10.5802/crgeos.99

Perspectives on alkaline magmas / *Perspectives sur les magmas alcalins*

Early carbonatite magmatism at Oldoinyo Lengai volcano (Tanzania): carbonatite–silicate melt immiscibility in Lengai I melt inclusions

Lydéric France [*, a], **Florian Brouillet** [a, b] **and Sarah Lang** [a, c]

[a] Université de Lorraine, CNRS, CRPG, F-54000 Nancy, France

[b] School of Earth and Environmental Sciences, University of St Andrews, St Andrews KY16 9AL, UK

[c] Department of Earth Sciences, Sapienza - University of Rome, P. le Aldo Moro 5, 00185 Roma, Italy

E-mails: lyderic.france@univ-lorraine.fr (L. France), fcgb1@st-andrews.ac.uk (F. Brouillet), sarah.lang@uniroma1.it (S. Lang)

Abstract. Carbonatites are unusual C-rich alkaline magmas that have been reported throughout the geological record. Nevertheless, there is only one currently active carbonatite system on Earth: Oldoinyo Lengai stratovolcano in northern Tanzania (God's mountain in Maasai culture). Present-day Lengai carbonatites are natrocarbonatites, peculiar Na-rich carbonatites that, under atmospheric conditions, alter and leach to compositions similar to the more common Ca-carbonatites within weeks, preventing any long-term geological record of such Na-rich magmas. It follows that the oldest report of natrocarbonatites at Oldoinyo Lengai dates to the 19th century. Here, by using samples from the Lengai I cone (>11 ka), we show that immiscible silicate–carbonatite melts were already present at reservoir conditions at that time. Measurements of three-phase (carbonatite + silicate + gas) melt inclusions from Lengai I highlight that their chemical compositions were similar to those of immiscible melts recently present in the reservoir. Alkaline carbonatites in melt inclusions from both Lengai I and historical explosive eruptions are enriched in Ca relative to those historically effused at the surface and likely record higher equilibrium temperatures (>1100 °C). We also report chemical maps that qualitatively document elemental partitioning between immiscible silicate–carbonatite melts. We show that at the melt inclusions' entrapment conditions Si, Fe, K, Na, and Cl are compatible with the silicate phase when C, Ca, P, Sr, Ba, and F are compatible with the carbonate phase.

Keywords. Carbonatite, Melt inclusion, Tanzania, Oldoinyo Lengai, Phonolite, Immiscibility.
Available online 8th December 2021

1. Introduction

Carbonatites are relatively rare magmas that contain >50% carbonate minerals [Le Bas et al., 1972] and, along with associated alkaline silicate magmas, constitute the main rare earth element (REE) deposits worldwide [e.g., Ling et al., 2013, Verplanck et al., 2014]. Although carbonatitic magmas are rare compared to silicate magmas, they have been produced throughout Earth's History, from the Archean

* Corresponding author.

to present day [Woolley and Kjarsgaard, 2008]. More than 500 occurrences have been reported globally; 35% in Africa, 30% in Asia, and 22% in North America [Woolley and Kjarsgaard, 2008]. Although reported in various geodynamic contexts, carbonatites are most commonly associated with rift environments; ~90% are intrusive and 80% are associated with alkaline silicate magmas [Woolley and Kjarsgaard, 2008].

Carbonatites are highly reactive at atmospheric conditions and alkali-rich compositions leach within weeks [Dawson et al., 1987, Zaitsev and Keller, 2006], making it highly challenging to identify the original chemical compositions of older deposits [e.g., Kogarko et al., 1991, Chen et al., 2013]. Although directly sampling fresh lava avoids this issue, only one carbonatitic volcano is presently active on Earth, the Oldoinyo Lengai [Tanzania; Dawson, 1962a]. The highly alkaline carbonatites that erupted there, natrocarbonatites, differ from the Ca-carbonatites that represent the overwhelming majority of fossil carbonatite occurrences. Nevertheless, the rare available data directly documenting carbonatite melt compositions (i.e., from melt inclusions that shelter carbonatites from surface weathering) indicate the alkaline character of parental carbonatite magmas in various regions [Kogarko et al., 1991, Mitchell, 2009, Sharygin et al., 2012, Chen et al., 2013, Guzmics et al., 2015, Mollex, 2017, Weidendorfer et al., 2017]. This raises the question of whether Ca-carbonatites effectively represent the magmatic composition or rather represent the leaching products of initially alkaline carbonatites [e.g., Dawson, 1962b, Hay, 1983, Keller and Zaitsev, 2006, Chen et al., 2013].

Traces of alkaline carbonatites have been identified at various sites: Oka carbonatite [Canada; Chen et al., 2013], Guli carbonatite [polar Siberia; Kogarko et al., 1991], and various volcanoes from the Natron Lake magmatic province in northern Tanzania, including Oldoinyo Lengai [Mitchell, 2009, Sharygin et al., 2012, Guzmics et al., 2015]. Although the volcano is famous worldwide for its natrocarbonatite emissions, such carbonatite products have only been reported for the most recent deposits and represent <5% of the Oldoinyo Lengai edifice [e.g., Klaudius and Keller, 2006]. This is likely due to how quickly natrocarbonatite lavas alter under atmospheric conditions. Nonetheless, the oldest report of natrocarbonatites can be attributed to the German missionaries Krapf and Erhardt, who reported snow at the summit of Oldoinyo Lengai in a map dated 14 March 1855 [Dawson et al., 1995a]; they likely misinterpreted the presence of snow, which is unlikely at such elevations in northern Tanzania, as altered natrocarbonatites, which are bright whitish and may resemble snow cover. The first known direct observation of what would later be called natrocarbonatites was by Uhlig [1905], who described "mudflows [...] covered with efflorescence of a white sodium salt". There is no direct evidence of any older carbonatite magmatism at Oldoinyo Lengai, and it is our aim to provide such evidence here.

Oldoinyo Lengai stratovolcano [edifice volume ~41 km^3; Kervyn et al., 2008] is in the Gregory rift, which forms the eastern branch of the East African rift. The oldest deposits of the volcano itself date to 350 ka [Sherrod et al., 2013] and form a phonolite cone comprising tuffs and lava flows (Lengai I, ~60% of the present-day edifice; Figure 1). After a major sector collapse before 11 ka [Kervyn et al., 2008, Sherrod et al., 2013], an alkaline-nephelinite cone comprising tuffs and lava flows grew [Lengai II, ~35% of the present-day cone; Figure 1; Klaudius and Keller, 2006]. During the last century, eruptive activity has consisted of decades of low-temperature, low-viscosity effusions of natrocarbonatite lava flows punctuated by sub-Plinian eruptions that emit both silicate (alkaline nephelinite and phonolite) and carbonatite magmas [Keller et al., 2010, Kervyn et al., 2010]. Although the genesis of carbonatites may be related to alternative processes in other geodynamic contexts [e.g., the direct formation of Ca-carbonatite from carbonated peridotites; Hammouda et al., 2014], Oldoinyo Lengai carbonatites are clearly related to liquid immiscibility between carbonatite and evolved silicate alkaline magmas [alkaline nephelinite and phonolite; e.g., Peterson, 1989, Fischer et al., 2009, Casola et al., 2020]. Indeed, conjugate carbonatite–silicate immiscible melts in melt inclusions (MIs) within various minerals from the 1917 and 2007–2008 explosive eruptions of Oldoinyo Lengai [e.g., Mitchell, 2009, Sharygin et al., 2012, de Moor et al., 2013, Mollex, 2017, Baudouin et al., 2020] attest to the coexistence of both melts within the Lengai reservoir and to their evolved character. Although carbonatites from MIs are less enriched in Na than erupted natrocarbonatites, they are alkali-rich and in equilibrium with their coexisting evolved silicate magmas, which are similar

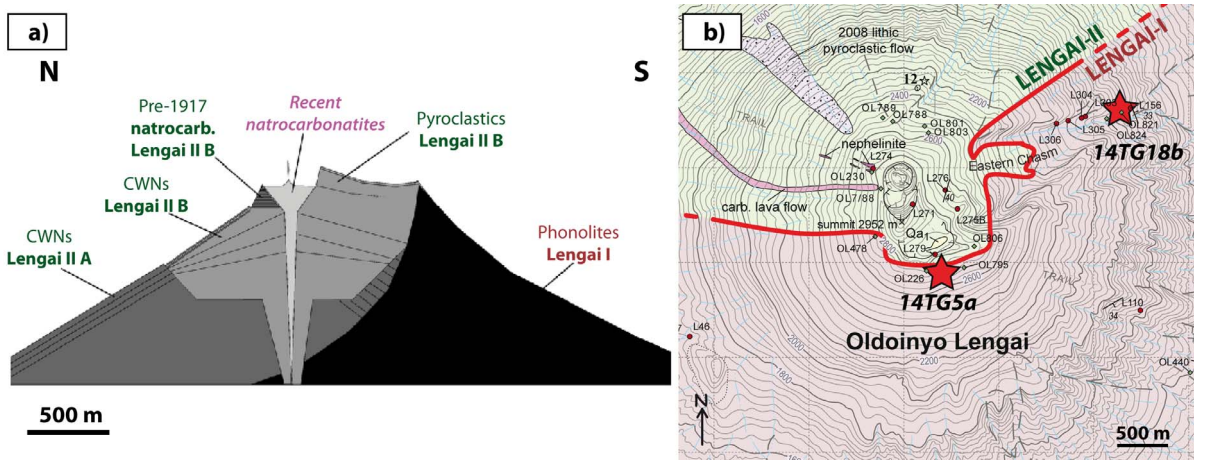

Figure 1. Sample setting and Oldoinyo Lengai architecture. (a) Synthetic N–S cross section highlighting the architecture of Oldoinyo Lengai stratovolcano, comprising >11 ka phonolite deposits of Lengai I to the south and combeite wollastonite nephelinite (CWN) and natrocarbonatite deposits of Lengai II to the north. This section is reproduced from Klaudius and Keller [2006]. (b) Map of the Oldoinyo Lengai summit area, showing the two sampling sites (red stars) from the present study. The limit between Lengai I and Lengai II (red line) proposed by Klaudius and Keller [2006] is also shown along with their sampling sites (used to define the delimitation) and those of Sherrod et al. [2013]. This map is modified from Sherrod et al. [2013].

to those of the older Lengai I and II deposits. This raises the question of whether immiscible carbonatites were present at the time of Lengai I and II, carbonatites that certainly would have weathered during their >11 ka of surface exposure. Here, we use nepheline-hosted MIs sampled from Lengai I phonolite lava flows (>11 ka) to demonstrate that carbonatite was present within the Lengai I reservoir and to document its composition.

2. Samples and petrography

2.1. *Phonolite lavas*

Two lava flows from the Lengai I edifice were sampled for the present study in two different areas of Lengai I cone. Sampling sites were selected based on the chemical architecture of Oldoinyo Lengai defined by Klaudius and Keller [2006], and we followed their sampling strategy (Table 1). Sample 14TG18bB was sampled at an elevation of 1678 m on the northeast flank of Oldoinyo Lengai, on the northern rim of the Eastern Chasm (Figure 1). Sample 14TG05a was sampled at ~2780 m elevation on the southern flank of the south crater, ~20 m·S below the southern rim (Figure 1). Both samples are massive porphyritic lava flows comprising microlite matrix (~50%), vesicles (~25%), and phenocrysts (~25%; Figure 2). Phenocrysts include colorless, euhedral nepheline (up to 5 mm; ~60% and 80% in 14TG18bB and 14TG05a, respectively), green, euhedral clinopyroxene (up to 3 mm; ~30% and 10% in 14TG18bB and 14TG05a, respectively), and subordinate Fe–Ti oxides (~8%), titanite (~1%), and melanite (Ti-garnet; ~1%). This mineral assemblage is characteristic of Oldoinyo Lengai phonolites and related ijolite cumulates [e.g., Dawson et al., 1995b, Klaudius and Keller, 2006, Mollex et al., 2018, Baudouin and France, 2019, Baudouin et al., 2020]. In both samples, clinopyroxene and nepheline host green composite MIs (Figure 3).

2.2. *Melt inclusions*

In both samples, MIs are oval to roundish, 10–40 μm wide, and commonly comprise three phases: green silicate glass, a carbonatite phase, and a shrinkage gas bubble (Figure 3). When only two phases are present, they are silicate glass and a shrinkage bubble. Because MIs are difficult to identify and describe

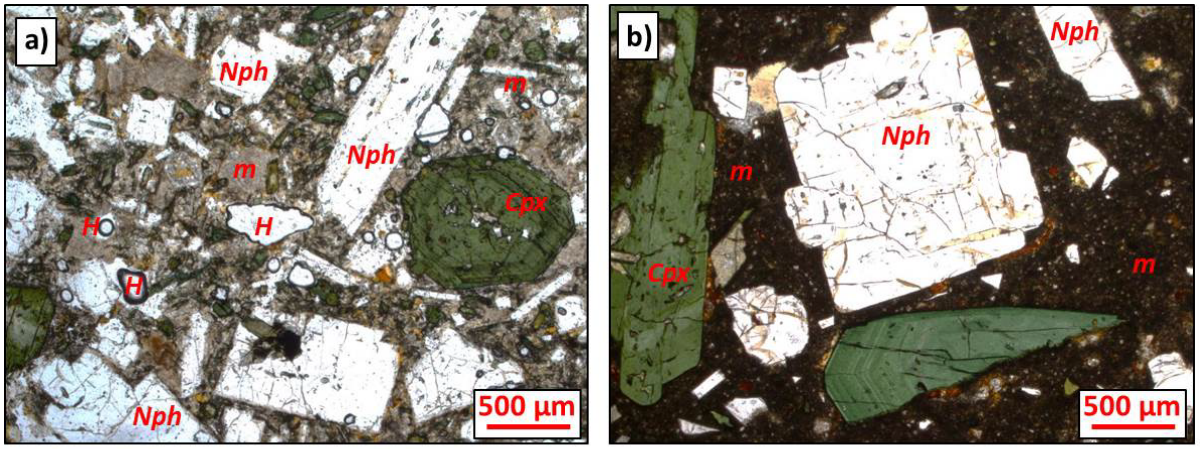

Figure 2. Microphotographs of phonolite lava flows studied herein (plane-polarized light): (a) sample 14TG05a and (b) sample 14TG18b. Cpx, clinopyroxene; Nph, nepheline; H, hole; m, matrix (microlites + crystallites + glass).

Table 1. Sample locations

Sample	Latitude	Longitude	Elevation	Location
14TG18b	2° 45′ 14.00″ S	35° 56′ 2.00″ E	1678 m	East flank
14TG05	2° 46′ 1.49″ S	35° 55′ 2.17″ E	2845 m	Southern flank of south crater

in similarly colored green clinopyroxenes, we focused on nepheline-hosted MIs. The carbonatite phase is either present as a spherical globule (Figure 3a, b) or a thin film wetting the shrinkage bubble (Figure 3c, d). Some inclusions contain silicate glass, a shrinkage bubble, and several carbonatite globules of various diameters (Figure 3e).

3. Methods

Whole-rock major and trace element concentrations of the two samples were determined by inductively coupled plasma optical emission spectrometry and inductively coupled plasma mass spectrometry, respectively at the Service d'Analyse des Roches et des Minéraux (SARM, CRPG, Nancy, France). Analyses were performed using HNO_3 solutions prepared from fused glass. Details of sample preparation, analytical settings and conditions, and detection limits, are reported in Carignan et al. [2001]. Analytical uncertainties are 2% and 5–10% for major and trace element concentrations, respectively.

MIs were studied both in thin sections and on separated grains. Separated grains containing three-phase MIs (gas, silicate, and carbonate) were picked under a binocular microscope and polished using Al disks to expose the inclusions; polishing was performed without water to prevent carbonate dissolution. Polished grains were then pressed into indium mounts. Thin sections were also prepared without water to prevent carbonate dissolution. Exposed inclusions were first imaged by scanning electron microscopy (SEM) to identify µm-sized carbonate phases in X-ray chemical maps. Because carbonates are commonly wetting gas bubbles, the carbonate layer is often too thin for EPMA (Electron Probe Microanalysis); only the compositions of carbonate layers thicker than 3 µm were tentatively quantified with EPMA.

Mineral major element compositions were determined using a CAMECA SX100 microprobe at the Service Commun de Microscopie Electronique et de Microanalyses X (SCMEM, Université de Lorraine, Nancy, France) equipped with five spectrometers and the "Peak sight" operating system. Analyses were performed using a 10 kV accelerating potential, a static (fixed) beam, Kα emissions for all elements, and a matrix correction based on Pouchou and Pichoir

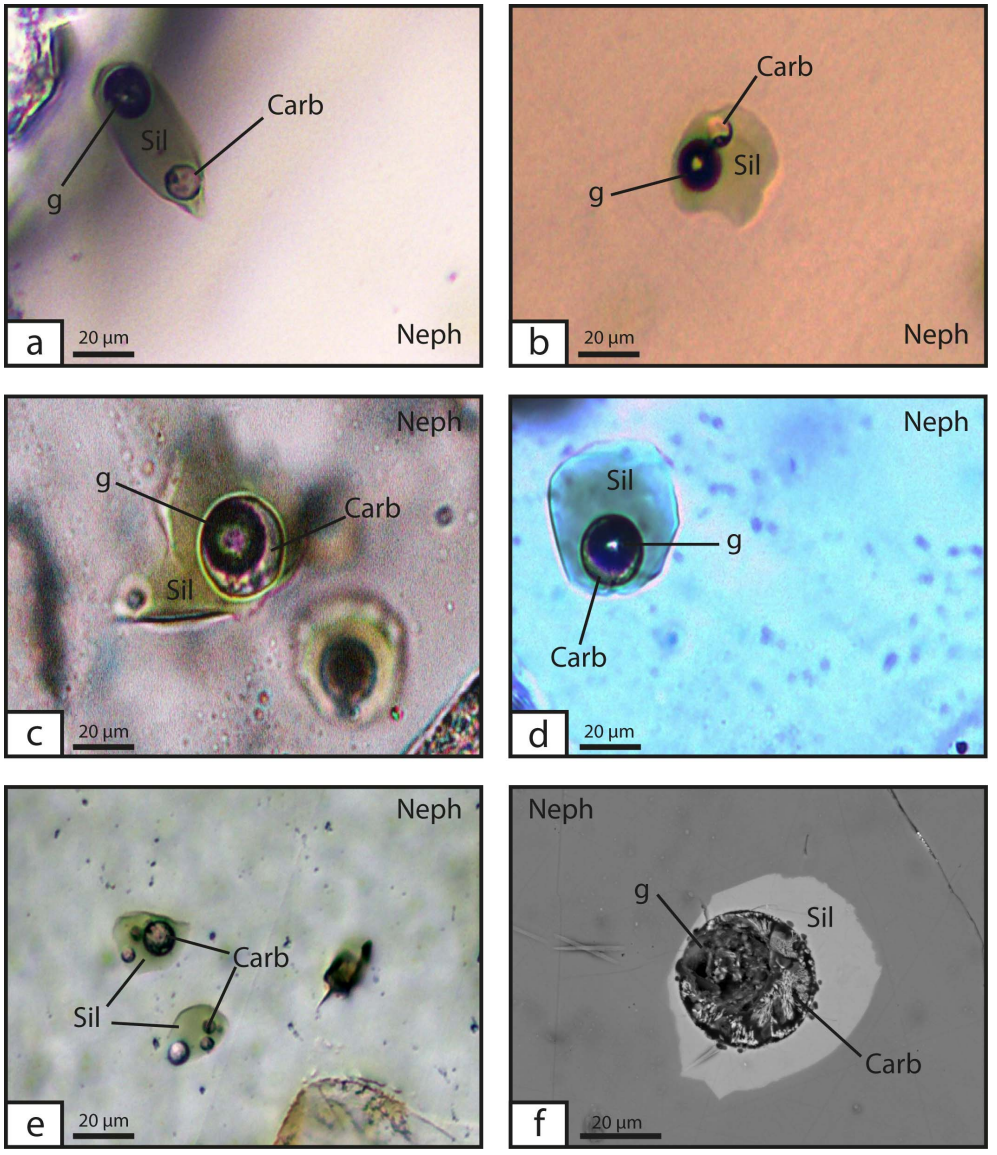

Figure 3. Microphotographs (a–e, sample 14TG18b) and backscattered electron image (f, sample 14TG05a) of nepheline-hosted three-phase melt inclusions containing silicate glass ("Sil"), carbonate "glass" ("Carb", actually microcrystalline as evident in (f)), and gas bubbles resulting from shrinkage ("g"). (a, b) Single, isolated carbonate globules in melt inclusions. (c, d, f) Carbonate melt rimming the gas bubble. (e) Multiple carbonate globules are present in some melt inclusions.

[1991]. Crystals were analyzed with a beam current of 10 nA using a focused beam and counting times of 20 s on background, and 40 s on peak (15 s for K and Na that were measured first). Both carbonate and silicate glasses were analyzed with a beam current of 5 nA using a defocused beam 3–15 µm in diameter depending on the size of the inclusion. To minimize elemental migration, background and peak counting times for inclusions were reduced to 10 s and 20 s, respectively (10 s on peak for K and Na, again measured first). In addition to in situ measurements, semi-quantitative chemical maps were obtained for

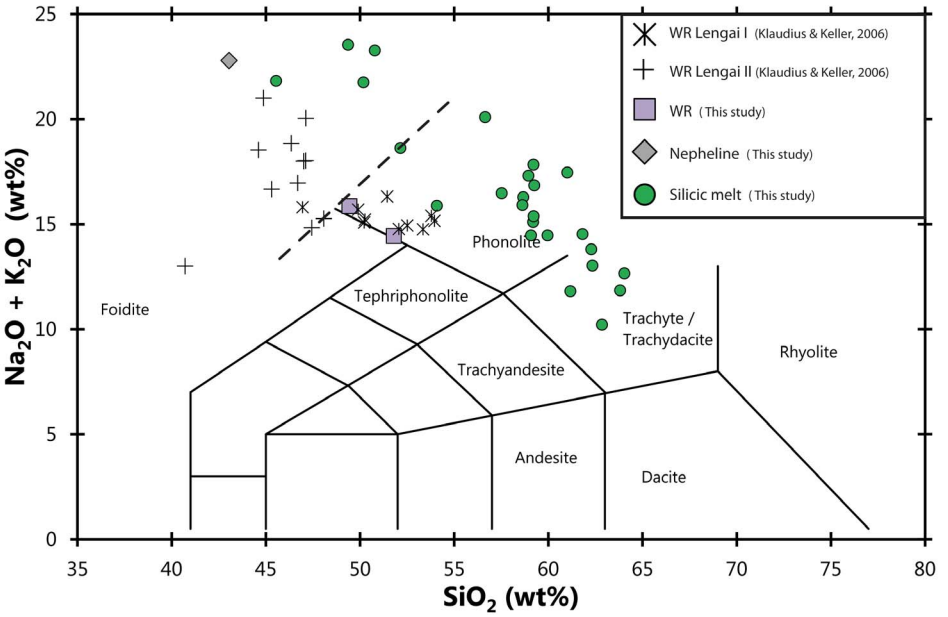

Figure 4. Total alkali versus silica diagram [after Le Maitre et al., 1989] showing the compositions of silicate melts from the Lengai I melt inclusions studied herein and the average composition of their host nephelines. Whole-rock (WR) compositions are also presented and compared to the Lengai I/II data of Klaudius and Keller [2006]. The samples studied herein are phonolites, compositionally similar to Lengai I deposits. The dashed line denotes the proposed division between the Foidite and Phonolite fields.

major elements and some trace elements (Ce, Ba, Sr, Cl, S, Mn) using a JEOL 7600F (Schottky field-emission gun) SEM equipped with an Oxford Instruments SDD-type energy dispersive spectrometer at the SCMEM. Chemical maps were acquired using an accelerating voltage of 15 kV, a beam current of 20 nA, and a dwell time of 24 ms/pixel, and data were deconvoluted pixel by pixel using the Oxford algorithm.

4. Chemical compositions

4.1. *Whole-rock compositions*

Whole-rock compositions (Table S1 in the supplementary materials) display relatively high loss on ignition (LOI), consistent with the relatively altered character of the rocks forming Oldoinyo Lengai stratovolcano [e.g., Klaudius and Keller, 2006]. Once recalculated on an anhydrous basis, the samples are classified as phonolites (Figure 4) with similar compositions to those defining the Lengai I series according to Klaudius and Keller [2006], confirming that the samples correspond to this oldest series (whereas the Lengai II series is relatively enriched in alkalis and depleted in silica). On average, the studied samples contain (once recalculated on a anhydrous basis) 50.6 wt% SiO_2, 17.6 wt% Al_2O_3, 7.8 wt%, Fe_2O_3 (total iron), 10 wt% Na_2O, 5 wt% K_2O, 5.7 wt% CaO, 1.2 wt% MgO, 1.2 wt% TiO_2, ~0.2 wt% Cl, and ~0.2 wt% F.

4.2. *Silicate glass compositions*

The studied inclusions are hosted in nepheline crystals with compositions characteristic of nephelines from Oldoinyo Lengai phonolites and related ijolite cumulates [Table 2; e.g., Dawson et al., 1995b, Klaudius and Keller, 2006, Bosshard-Stadlin et al., 2014, Mollex, 2017, Berkesi et al., 2020]. Silicate glasses range in composition from trachyte to phonolite (Figure 4) with alkaline contents varying from ~10 wt% to more than 20 wt%. Some rare MIs are particularly enriched in K_2O (up to 9.5 wt%, Figure 5). On average, silicate glasses contain 54 ± 4.5 wt% SiO_2, 11.1 ± 2.1 wt% Na_2O, 11 ± 1.5 wt% FeO (total iron), 5.3 ± 1.0 wt% CaO, 4.3 ± 1.1 wt% Al_2O_3, 4.3 ± 2.7 wt% K_2O, 1.4 ± 0.3 wt% TiO_2, 0.65 ± 0.2

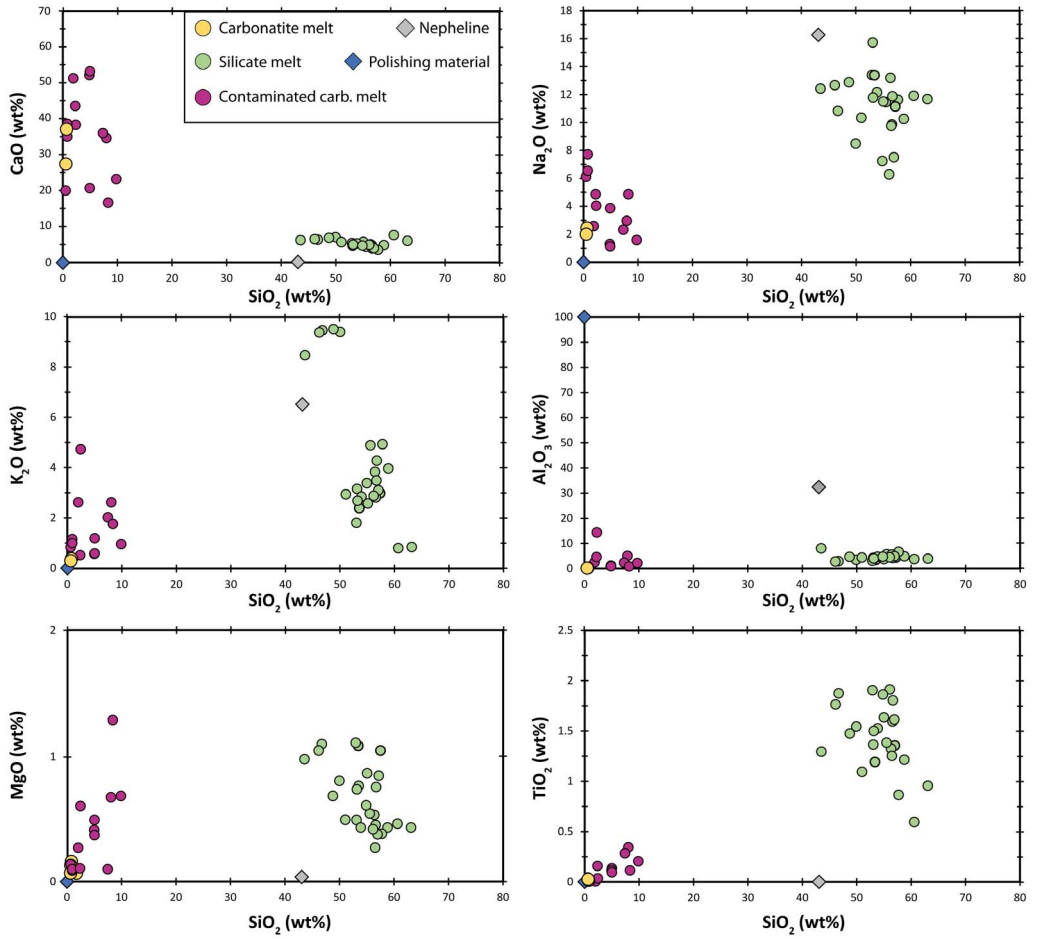

Figure 5. Chemical compositions of three-phase melt inclusions from Lengai I phonolite lava flows. Grains were polished with Al-discs to prevent carbon contamination, and we document the composition of the polishing material as a potential contaminant of the measurements. The two yellow circles ("Carbonatite melt") are considered to be representative of the carbonatite phase composition because those data were obtained on portions of carbonatite large enough to ensure accurate measurements. Other data (purple circles, "Contaminated carb. melt") were measured on smaller carbonatite globules and likely represent carbonatite analyses that included some portion(s) of silicate melt, the host nepheline, and/or polishing material.

wt% MgO, 1.3 ± 0.4 wt% F, 0.8 ± 0.4 wt% SO_2, and 0.5 ± 0.2 wt% Cl (Table 2, Figures 4 and 5). Silicate glass from two-phase and three-phase melt inclusions display similar chemical compositions. The chemical trend defined by the silicate glass major element contents does not align with the host nepheline composition (Figure 5); therefore, the corresponding chemical variability is not related to post-entrapment processes. The silicate glasses in nepheline-hosted MIs studied herein are similar to those reported in MIs from the 1917 Oldoinyo Lengai explosive eruption (Figure 6; 1917 data from Sharygin et al. [2012] are represented by a brown square in Figure 6).

4.3. *Carbonate "glass" composition*

It is very challenging to accurately determine the compositions of carbonatite globules in the composite nepheline-hosted MIs because the carbon-

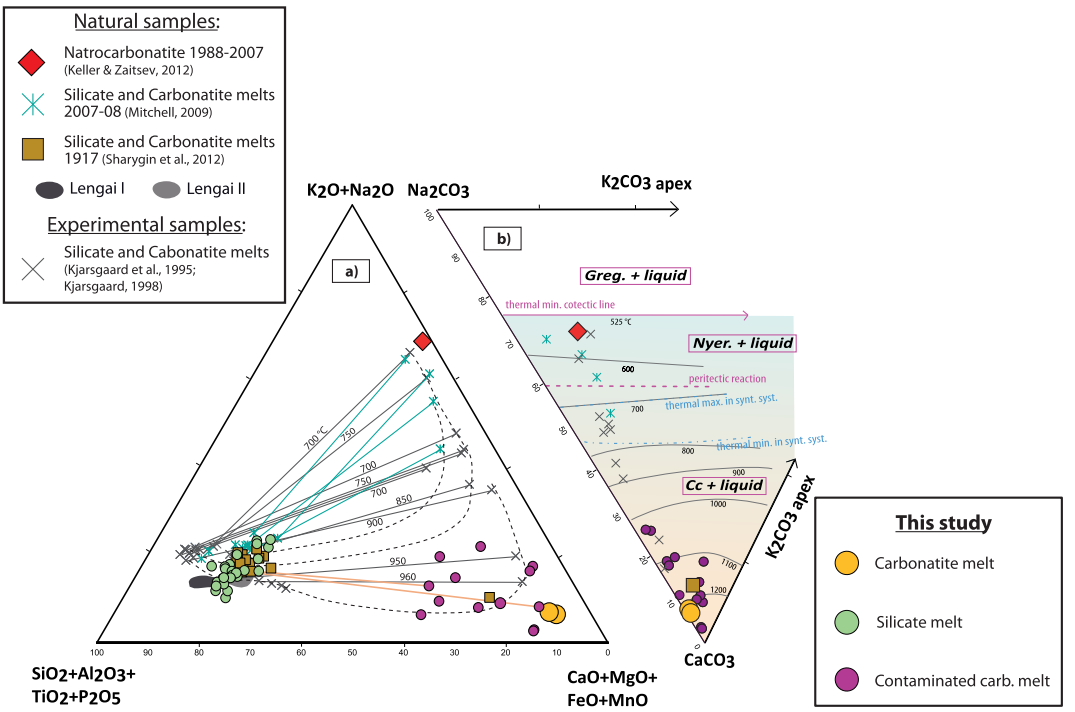

Figure 6. (a) Pseudoternary multicomponent diagram grouping the network forming elements (bottom left), network modifying elements (bottom right), and alkalis [top; after Freestone and Hamilton, 1980]. The silicate and carbonatite melts from the present study are compared to the average natrocarbonatite composition of Keller and Zaitsev [2012], the compositions of immiscible silicate and carbonatite melts in melt inclusions from the 1917 [Sharygin et al., 2012] and 2007–2008 eruptions [Mitchell, 2009], and the compositions of experimental silicate–carbonatite melt pairs [only data for pressures <4 kbar are shown; Kjarsgaard et al., 1995, Kjarsgaard, 1998]. Dashed curves represent the extent of the miscibility gap as a function of increasing peralkalinity. Solid lines are tie lines between conjugate natural and experimental melts; numbers adjacent to experimental tie lines indicate the corresponding equilibrium temperature (°C). (b) Carbonatite melts plotted on the Na–K–Ca-carbonate ternary of Cooper et al. [1975]. Liquidus surfaces are derived from Weidendorfer et al. [2017] and are valid for the natural system. The thermal minimum, thermal maximum, and peritectic reactions are from Cooper et al. [1975]; they apply to the synthetic system and are presented for comparison. Cc, calcite; Greg., gregoryite; Nyer., nyerereite.

atites are finely crystallized, are usually present in the form of a thin micron-thick film wetting the shrinkage bubble rims, and because some of the polishing material (Al-rich) regularly fills the bubble cavities. For these reasons, chemical maps are particularly valuable for identifying carbonatite melts (Figure 7). Also, chemical maps are useful because the intensity contrast between the silicate and carbonatite melts highlights the partitioning behavior of various chemical elements between the two melts (Figure 8). Ca-rich, Si-poor globules within the silicate MIs (Figure 7) correspond to the visually identified carbonatite globules (Figure 3). Detailed maps highlight that the carbonatite melts are depleted in Si, K, Fe, Na, and Cl and enriched in C, Ca, P, F, Sr, and Ba compared to the silicate MIs (Figures 7, 8). Although challenging, in situ measurements of very rare large inclusions (e.g., Figure 3f) provide some quantitative compositions that can be used herein as a reference (Figure 5). Other carbonatite globule measurements were contaminated by either the silicate melt, some polishing material trapped in the

bubble cavity, or the host nepheline. The least contaminated measurements are reported for comparison in Figure 5 and allow us to better discuss the accurate measurements (e.g., depletion in Na of the carbonatite relative to the silicate melt).

5. Discussion

5.1. *Carbonatite magma was already present during early Oldoinyo Lengai evolution*

The results presented herein clearly document the presence of carbonatite–silicate melt immiscibility in nepheline-hosted MIs from Lengai I products. The presence of carbonatites within the Lengai I MIs is at odds with the lack of such magmas in the geological record of the Lengai I cone, but is likely explained by the fact that MIs are shielded from the atmosphere, and therefore from leaching. Nevertheless, before we can conclude that those immiscible melts were present within the magma reservoir >11 ka, we must first discuss the potential effect of post-entrapment crystallization on the bulk compositions of the inclusions [e.g., Rose-Koga et al., 2021]. Given the compositions of the host nepheline phenocrysts, post-entrapment crystallization should result in an overall increase in the Si content and decreases in the Na and K contents of the bulk MIs. According to experimental constraints and related applications to natural systems, such compositional variations would shift the bulk compositions of the inclusions out of the miscibility gap [Kjarsgaard and Peterson, 1991, Martin et al., 2013, Weidendorfer et al., 2016, 2017, Schmidt and Weidendorfer, 2018]. Thus, the effects of post-entrapment crystallization would diminish, not enhance, any evidence of carbonate–silicate immiscibility. Our results thus clearly demonstrate that immiscible carbonatite and silicate melts were present at depth within the Lengai I magmatic reservoir >11 ka.

The carbonatite component in the Lengai I MIs is an alkaline Ca-carbonatite (up to 37 wt% CaO, ~2 wt% Na_2O; Figure 6; Table 2). It is less sodic and more calcic than (i) the natrocarbonatites historically erupted at Oldoinyo Lengai [15.6 wt% CaO, ~32 wt% Na_2O; Keller and Zaitsev, 2012] and (ii) the alkaline carbonatites present as immiscible melts within MIs from the most recent sub-Plinian eruption of Oldoinyo Lengai in 2007–2008 [18.3 wt% CaO, 26.3 wt% Na_2O; e.g., Mitchell, 2009, Mollex, 2017]. It is, however, similar to the immiscible alkaline carbonatite melts reported within MIs from the 1917 sub-Plinian eruption of Oldoinyo Lengai [~37 wt% CaO, 3.4 wt% Na_2O; Sharygin et al., 2012]. Experimental results have demonstrated that carbonatites become less calcic and more sodic with decreasing temperature during magma differentiation [Figure 6; Kjarsgaard et al., 1995, Kjarsgaard, 1998, Weidendorfer et al., 2017, Nabyl et al., 2020]. These results strongly suggest that the alkaline carbonatites present within the igneous reservoir during the Lengai I stage (this study) or during the 1917 eruption [Sharygin et al., 2012] were equilibrated at higher temperatures than those present in the reservoir during the 2007–2008 eruption [Mitchell, 2009] or erupted at surface during historical times [Keller and Zaitsev, 2012]. The phase diagram shown in Figure 6 highlights that the equilibrium temperatures of the Lengai I alkaline Ca-carbonatites were likely 1100–1200 °C [Weidendorfer et al., 2017], consistent with the minimum temperature of 1130 °C obtained by Sharygin et al. [2012] for the entrapment conditions of the 1917 MIs based on a thermometric approach. Furthermore, Baudouin et al. [2020]; using the clinopyroxene-melt thermometer of Masotta et al. [2013] obtained lower equilibrium temperatures of 930–1060 °C for 2007–2008 ijolite samples containing MIs similar to those described by Mitchell [2009]. Those equilibrium temperatures are much higher than the eruptive temperatures reported for historical natrocarbonatites, 490–600 °C [Keller and Krafft, 1990, Dawson et al., 1995b], temperatures that are again consistent with phase diagram constraints [Figure 6; Weidendorfer et al., 2017].

These results support that high-temperature (>900 °C), immiscible, alkali-poor alkaline carbonatites are present at reservoir depth, whereas cooler, alkali-rich natrocarbonatites are emitted during present-day surface eruptions. The transition from ~900 °C alkaline carbonatites to <600 °C natrocarbonatites is not directly documented herein, but has been shown to be feasible during the protracted differentiation of magmas compositionally similar to those of the Natron Lake igneous province [Weidendorfer et al., 2017]. Such protracted differentiation likely occurred at reservoir conditions or during magma ascent.

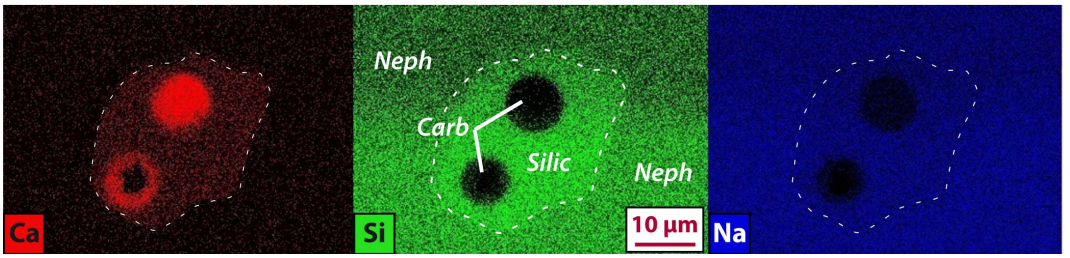

Figure 7. Ca, Si, and Na chemical maps for a three-phase melt inclusion hosted in a nepheline crystal ("Neph") in sample 14TG18b. Two Ca-rich, Si-poor carbonatite globules ("Carb") are present within the silicate melt ("Silic"). The white dashed line delimits the melt inclusion.

Our new results eventually highlight the coexistence of alkaline carbonatite and alkaline silicate melts in the igneous reservoir during the Lengai I period (>11 ka), and thus document a similar igneous configuration than during historical eruptions. We can thus propose here that although there is no direct evidence that alkaline carbonatites or natrocarbonatites were erupted during the Lengai I period, carbonatite eruptions similar to the present-day ones most likely occurred at that time.

5.2. *Implications for elemental partitioning between immiscible silicate–carbonatite melts*

Direct compositional measurements of carbonatite globules are very challenging, and we are unable to provide quantitative data on elemental partitioning between immiscible silicate–carbonatite melts (see Sections 3 and 4.3). Nevertheless, chemical maps of the composite MIs qualitatively characterize the behaviors of various elements, and we here estimate the pressure–temperature conditions for which those partitioning constraints are valid. The chemical compositions of the identified carbonatites and previous experimental results strongly suggest that the equilibrium temperatures of the studied immiscible melts were 1100–1200 °C (e.g., Figure 6, see Section 5.1). The pressure conditions preserved by MIs roughly correspond to the entrapment pressure, which is likely the reservoir depth. At Oldoinyo Lengai, the recent upper crustal reservoir is likely at 10–15 km depth, corresponding to pressures of 3–5 kbar [Baer et al., 2008, Albaric et al., 2010, Mollex, 2017]. Given that magmatic compositions during the Lengai I period were quite similar to those evidenced by historical eruptions, we expect that the plumbing system architecture was also largely similar. Therefore, the partitioning constraints provided hereafter are valid for such pressure–temperature conditions (3–5 kbar, 1100–1200 °C). Chemical maps presented in Figures 7 and 8 highlight that Si, Fe, and K are preferentially incorporated into the silicate melt whereas C, Ca, P, Sr, and Ba are preferentially incorporated in the carbonate melt, consistent with previous natural and experimental data [Hamilton et al., 1989, Jones et al., 1995, Veksler et al., 1998, 2012, Guzmics et al., 2012, Martin et al., 2013]. Notably, our results show that Na, which has been reported as compatible with the carbonate melt in most experimental studies, is rather slightly enriched in the silicate melt at the studied conditions (Figures 5, 7). Similar preferential incorporation of Na in the silicate melt has nevertheless been reported in some experiments by Kjarsgaard et al. [1995], Kjarsgaard [1998], and Nabyl et al. [2020], but there is no evident relation between this behavior and specific temperature and pressure conditions, or with composition. Fewer literature data are available for halogens; our results highlight that F strongly partitions into the carbonate phase, consistent with Kjarsgaard et al. [1995], Kjarsgaard [1998], Guzmics et al. [2012], Nabyl et al. [2020], whereas Cl rather partitions into the silicate melt. This latter result is consistent with previous experimental constraints as although Kjarsgaard et al. [1995], Kjarsgaard [1998], and Nabyl et al. [2020] have shown that Cl is compatible with the carbonate in most cases, partition coefficients as low as 0.6 were reported for some experiments. Again there is no evident relation between this behavior and specific temperature and pressure conditions, or

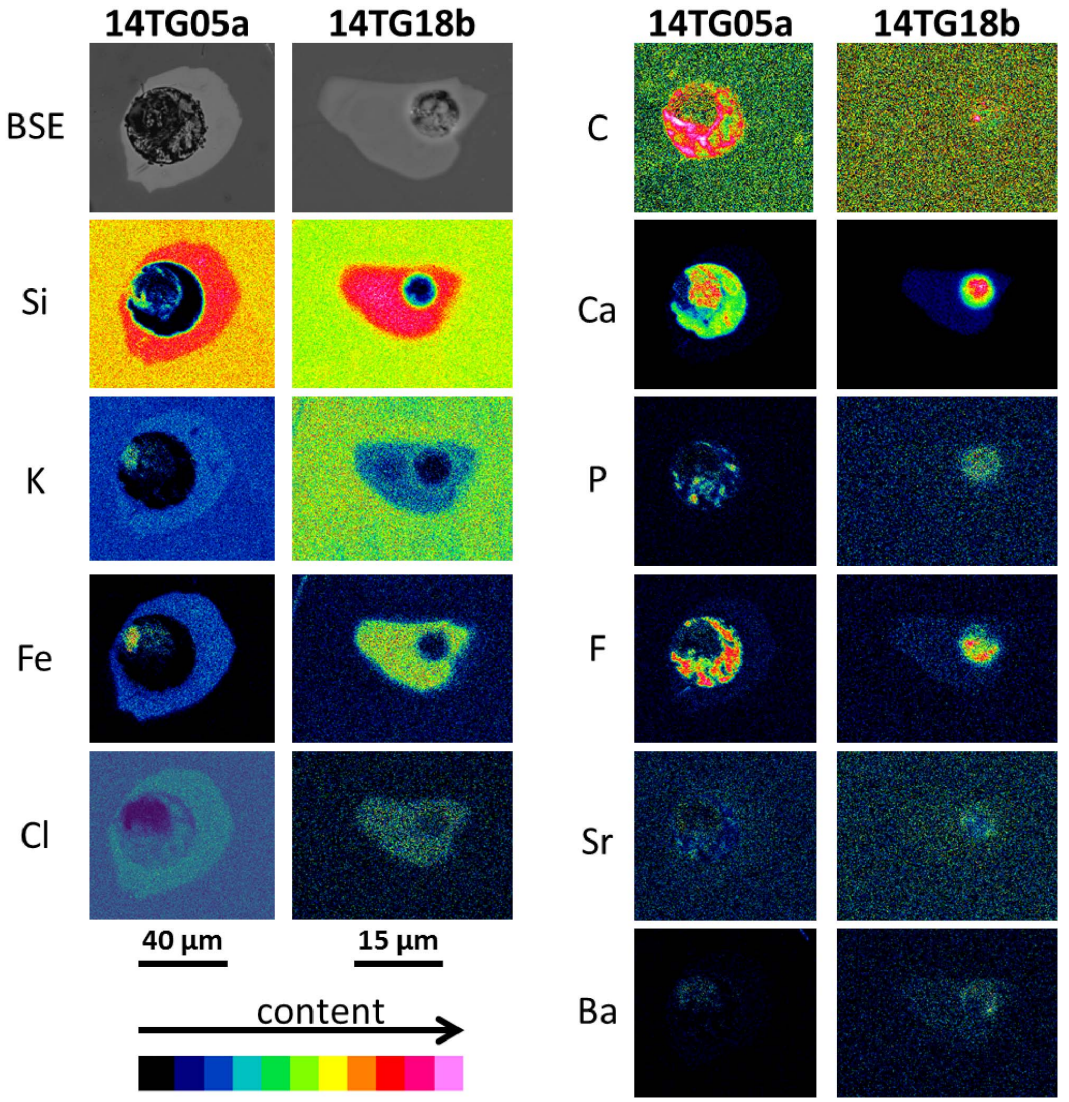

Figure 8. Backscattered electron (BSE) images and chemical maps for various elements in three-phase nepheline-hosted melt inclusions from two Lengai I samples. These maps qualitatively show elemental partitioning behaviors between immiscible silicate and carbonatite melts. Si, K, Fe, and Cl are enriched in the silicate relative to the carbonatite phase, whereas C, Ca, P, F, Sr, and Ba are enriched in the carbonatite relative to the silicate phase.

with composition, and further experimental work dedicated to the study of halogens partitioning between immiscible carbonatite–silicate melts would be required to better understand Cl behavior.

6. Summary

Oldoinyo Lengai is currently the only active carbonatite volcano worldwide, but the oldest previous evidence of carbonatite magmas there dates only to the 19th century. Here, based on nepheline-hosted melt inclusions that preserve immiscible carbonatite and conjugate silicate melts from surface weathering and leaching, we reported evidence of carbonatite magmas predating 11 ka at Oldoinyo Lengai. These newly identified carbonatites are enriched in Ca and depleted in Na compared to the modern natrocarbonatites historically emitted at the summit. In contrast

Table 2. Phase compositions (wt%)

Phase	Measurement no	SiO_2	TiO_2	Al_2O_3	FeO_t	MnO	MgO	CaO	Na_2O	K_2O	P_2O_5	F	SO_2	Cl	Total
Silicate melt	14TG18b_S03	57.21	1.35	4.27	11.27	0.40	0.85	5.18	11.02	2.99	0.13	1.12	0.58	0.47	96.84
Silicate melt	14TG18b_S04	53.53	1.21	3.04	16.10	0.35	0.77	5.37	13.38	2.34	0.27	1.58	0.60	0.43	98.97
Silicate melt	14TG05A_C020	43.56	1.29	7.88	10.81	0.44	0.98	6.22	12.40	8.47	0.41	2.14	0.86	0.17	95.63
Silicate melt	14TG05A_S05	49.99	1.54	3.38	12.35	0.25	0.81	7.06	8.46	9.40	0.16	1.52	0.63	0.30	95.85
Silicate melt	14TG05A_S06	60.66	0.59	3.64	9.07	0.04	0.47	7.63	11.88	0.80	0.17	1.20	0.25	0.74	97.14
Silicate melt	14TG05A_S07	63.15	0.95	3.81	9.18	0.58	0.44	6.06	11.65	0.84	0.00	0.74	0.33	0.90	98.63
Silicate melt	14TG18b_S08	58.84	1.21	4.73	10.82	0.50	0.44	4.83	10.23	3.97	0.10	1.18	0.58	0.51	97.94
Silicate melt	14TG05A_1-04	46.74	1.87	2.77	12.85	0.72	1.10	6.36	10.80	9.46	0.34	n.a.	1.82	0.25	95.08
Silicate melt	14TG05A_1-05	46.17	1.76	2.67	12.55	0.61	1.05	6.48	12.64	9.38	0.23	n.a.	1.87	0.28	95.69
Silicate melt	14TG05A_1-07	48.78	1.47	4.49	10.72	0.55	0.69	6.86	12.85	9.51	0.15	n.a.	0.79	0.34	97.20
Silicate melt	14TG18b_4-2	53.12	1.36	4.13	10.54	0.57	0.50	4.63	15.69	3.16	0.09	n.a.	0.87	0.48	95.14
Silicate melt	14TG18b_3-2	56.39	1.32	4.17	10.04	0.50	0.54	5.07	13.16	3.83	0.12	n.a.	0.71	0.45	96.30
Silicate melt	14TG18b_5-2	57.77	0.86	6.49	8.53	0.52	0.39	3.51	11.61	4.93	0.10	n.a.	0.23	0.39	95.33
Silicate melt	14TG18b_7-2	52.98	1.90	2.94	11.73	0.75	1.11	5.36	13.37	1.81	0.17	n.a.	1.22	0.57	93.91
Silicate melt	14TG18b_8-1	55.56	1.38	5.52	10.08	0.40	0.55	4.37	11.43	4.89	0.10	n.a.	1.05	0.59	95.92
Silicate melt	14TG18b_10-1	55.08	1.63	3.60	11.07	0.81	0.87	5.73	11.48	2.58	0.21	n.a.	1.02	0.66	94.74
Silicate melt	14TG18b_19-2	56.65	1.59	4.08	10.22	0.37	0.46	4.72	9.83	3.49	0.16	n.a.	0.86	0.45	92.88
Silicate melt	14TG18b_18-2	56.73	1.80	4.95	10.74	0.56	0.76	3.86	11.85	4.28	0.18	n.a.	0.98	0.57	97.26
Silicate melt	14TG18b_43_Si	53.92	1.52	4.57	10.57	0.45	0.44	5.27	12.12	2.85	0.17	0.79	0.22	0.34	93.23
Silicate melt	14TG18b_44_Si	56.54	1.25	5.39	9.70	0.46	0.28	4.60	9.73	2.82	0.07	1.56	0.42	0.34	93.15
Silicate melt	14TG18b_36_Si	51.05	1.09	4.24	9.47	0.49	0.50	5.69	10.31	2.94	0.37	1.42	0.73	0.50	88.81
Silicate melt	14TG18b_37_Si	53.20	1.50	3.88	11.09	0.66	0.74	4.97	11.76	2.68	0.26	1.12	0.53	0.54	92.92
Silicate melt	14TG18b_39_Si3	57.01	1.61	4.75	10.63	0.41	0.39	3.98	7.49	3.10	0.00	1.43	0.95	0.56	92.30
Silicate melt	14TG18b_19_Si	56.15	1.91	4.31	11.87	0.67	0.43	4.92	6.26	2.88	0.00	0.51	0.95	0.43	91.27
Silicate melt	14TG18b_17_Si	54.89	1.86	4.58	11.80	0.48	0.62	4.70	7.21	3.39	0.23	2.05	0.21	0.59	92.60
Carbonatite melt	14TG05A_1-02	0.73	0.01	0.05	0.17	0.06	0.17	37.06	2.41	0.38	2.24	n.a.	0.13	0.18	43.59
Carbonatite melt	14TG05A_1-03	0.61	0.02	0.00	0.11	0.00	0.14	27.38	1.97	0.29	2.03	n.a.	0.14	0.16	32.85
Contam. carb. melt	14TG18b_19-1	1.96	0.00	2.33	0.52	0.00	0.28	51.26	2.56	2.62	1.73	n.a.	0.21	1.05	64.52
Contam. carb. melt	14TG18b_18-1	2.39	0.03	14.24	0.32	0.17	0.61	38.31	4.01	4.73	2.69	n.a.	0.44	0.98	68.92
Contam. carb. melt	14TG18b_9-1	8.01	0.34	4.90	1.28	0.03	0.68	34.61	2.94	2.62	3.51	n.a.	0.41	0.85	60.18
Contam. carb. melt	14TG18b_12-2	7.39	0.28	2.20	1.85	0.19	0.11	35.97	2.30	2.03	1.75	n.a.	0.29	0.42	54.78
Contam. carb. melt	14TG05A_C014	0.85	0.00	0.00	0.00	0.10	0.10	38.57	7.69	1.16	2.25	23.69	0.06	0.10	74.57
Contam. carb. melt	14TG05A_C015	0.55	0.04	0.15	0.00	0.00	0.15	20.00	6.09	0.83	3.69	4.05	0.35	0.13	36.03
Contam. carb. melt	14TG05A_C017	8.32	0.11	0.72	0.00	0.01	1.29	16.66	4.84	1.76	5.03	0.14	0.27	0.08	39.23
Contam. carb. melt	14TG05A_C018	4.97	0.13	1.00	0.00	0.09	0.50	20.66	3.84	1.19	1.56	11.06	0.21	0.07	45.28
Contam. carb. melt	14TG05A_C021	0.85	0.01	0.13	0.00	0.00	0.11	35.04	6.53	1.00	2.33	23.78	0.11	0.11	70.00
Contam. carb. melt	14TG18b_C029	4.91	0.11	0.84	0.00	0.12	0.42	52.14	1.27	0.57	2.37	11.56	0.29	0.11	74.71
Contam. carb. melt	14TG18b_C030	4.98	0.09	0.76	0.14	0.00	0.38	53.18	1.10	0.59	2.74	12.06	0.45	0.11	76.58
Contam. carb. melt	14TG18b_C033	9.83	0.20	2.06	0.00	0.00	0.69	23.22	1.57	0.96	1.23	2.62	0.36	0.28	43.02
Contam. carb. melt	14TG18b_39_c2	2.32	0.15	4.45	0.58	0.06	0.12	43.54	4.84	0.52	3.02	19.36	0.28	0.66	79.88
Average nepheline		42.7	0.01	31.8	1.82	0.02	0.02	0.09	15.9	7.6	0.00	—	—	—	99.90

Contaminated carbonatite melt ("contam. carb. melt") indicates analyses of carbonatite melt that may have included adjacent silicate melt, host nepheline, and/or polishing material (see Sections 3 and 4.3). FeO_t is for total iron expressed as FeO.

they are similar to carbonatites that were recently present in the upper crustal igneous reservoir and preserved in melt inclusions from recent explosive eruptions. By comparison with previous experimental results, we suggest that this discrepancy highlights the presence of Ca-rich, Na-poor carbonatites at reservoir conditions (>1100 °C), which then differentiate to Na-rich, Ca-poor compositions during their ascent to the surface and related cooling. We also provide new qualitative data on elemental partitioning between immiscible carbonate and silicate melts.

Conflicts of interest

Authors have no conflict of interest to declare.

Acknowledgments

Céline Baudouin is thanked for numerous discussions about the Oldoinyo Lengai system and alkaline magmatism. Marine Boulanger is thanked for discussions and sample preparation advice. Andreï Lecomte and Jean Cauzid are thanked for assistance

with acquiring chemical maps and signal deconvolution. Gaëlle Mollex, Gilles Chazot, Pete Burnard, and Emmanuel Kazimoto are thanked for assistance and discussions during field work. We thank the two anonymous reviewers for their constructive comments, and Bruno Scaillet for his editorial handling and for his invitation to contribute to this special issue "Perspectives on alkaline magmas". We also thank the Tanzania Commission for Science and Technology (COSTECH) for field permits and all the guides and porters for their help during field work. This work was supported by the French National Research Agency through the national program "Investissements d'avenir" with the reference ANR-10-LABX-21-01/LABEX RESSOURCES21, and through the project GECO-REE (ANR-16-CE01-0003-01; P.I., Lydéric France). This study was also supported by the Région Lorraine, and PNP and CESSUR programs from INSU-CNRS (grants to Lydéric France). This is CRPG contribution number 2810 and GECO-REE contribution number 5.

Supplementary data

Supporting information for this article is available on the journal's website under https://doi.org/10.5802/crgeos.99 or from the author.

References

Albaric, J., Perrot, J., Déverchère, J., Deschamps, A., Le Gall, B., Ferdinand, R. W., Petit, C., Tiberu, C., Sue, C., and Songo, M. (2010). Contrasted seismogenic and rheological behaviours from shallow and deep earthquake sequences in the North Tanzanian Divergence, East Africa. *J. Afr. Earth Sci.*, 58(5), 799–811.

Baer, G., Hamiel, Y., Shamir, G., and Nof, R. (2008). Evolution of a magma-driven earthquake swarm and triggering of the nearby Oldoinyo Lengai eruption, as resolved by InSAR, ground observations and elastic modeling, East African Rift, 2007. *Earth Planet. Sci. Lett.*, 272(1-2), 339–352.

Baudouin, C. and France, L. (2019). Trace element partitioning between wollastonite and alkaline silicate magmas. *Chem. Geol.*, 523, 88–94.

Baudouin, C., France, L., Boulanger, M., Dalou, C., and Devidal, J. L. (2020). Trace element partitioning between clinopyroxene and alkaline magmas. *Contrib. Mineral. Petrol.*, 175, article no. 42.

Berkesi, M., Bali, E., Bodnar, R. J., Szabó, A., and Guzmics, T. (2020). Carbonatite and highly peralkaline nephelinite melts from Oldoinyo Lengai volcano, Tanzania: The role of natrite-normative fluid degassing. *Gondwana Res.*, 85, 76–83.

Bosshard-Stadlin, S. A., Mattsson, H. B., and Keller, J. (2014). Magma mixing and forced exsolution of CO_2 during the explosive 2007–2008 eruption of Oldoinyo Lengai (Tanzania). *J. Volcanol. Geotherm. Res.*, 285, 229–246.

Carignan, J., Hild, P., Mevelle, G., Morel, J., and Yeghicheyan, D. (2001). Routine analyses of trace element in geological samples using flow injection and low pressure on-line liquid chromatography coupled to ICP-MS: a study of geochemical reference materials BR, DR-N, UB-N, AN-G and GH. *Geostand. Newsl.*, 25, 187–198.

Casola, V., France, L., Galy, A., Bouden, N., and Villeneuve, J. (2020). No evidence for carbon enrichment in the mantle source of carbonatites in eastern Africa. *Geology*, 48, 971–975.

Chen, W., Kamenetsky, V. S., and Simonetti, A. (2013). Evidence for the alkaline nature of parental carbonatite melts at Oka complex in Canada. *Nat. Commun.*, 4, article no. 2687.

Cooper, A. F., Gittins, J., and Tuttle, O. F. (1975). The system Na_2CO_3–K_2CO_3–$CaCO_3$ at 1 kilobar and its significance in carbonatite petrogenesis. *Am. J. Sci.*, 275, 534–560.

Dawson, J. B. (1962a). Sodium carbonate lavas from Oldoinyo Lengai, Tanganyika. *Nature*, 195, 1075–1076.

Dawson, J. B. (1962b). The geology of Oldoinyo Lengai. *Bull. Volcanol.*, 24, 348–387.

Dawson, J. B., Garson, M. S., and Roberts, B. (1987). Altered former alkalic carbonatite lava from Oldoinyo Lengai, Tanzania: inferences for calcite carbonatite lavas. *Geology*, 15, 765–768.

Dawson, J. B., Keller, J., and Nyamweru, C. (1995a). Historic and recent eruptive activity of Oldoinyo Lengai. In Bell, K. and Keller, J., editors, *Carbonatite Volcanism: Oldoinyo Lengai and the Petrogenesis of Natrocarbonatites. IAVCEI Proc Volcanol 4*, pages 4–22. Springer, Berlin, Heiderlberg.

Dawson, J. B., Pinkerton, H., Norton, G. E., Pyle, D. M., Browning, P., Jackson, D., and Fallick, A. E. (1995b). Petrology and geochemistry of Oldoinyo Lengai lavas extruded in november 1988: magma source, ascent and crystallization. In Bell, K. and

Keller, J., editors, *Carbonatite Volcanism. IAVCEI Proceedings in Volcanology*, volume 4, pages 44–69. Springer, Berlin, Heidelberg.

de Moor, J. M., Fischer, T. P., King, P. L., Botcharnikov, R. E., Hervig, R. L., Hilton, D. R., Barry, P. H., Mangasini, F., and Ramirez, C. (2013). Volatile-rich silicate melts from Oldoinyo Lengai volcano (Tanzania): Implications for carbonatite genesis and eruptive behavior. *Earth Planet. Sci. Lett.*, 361, 379–390.

Fischer, T. P., Burnard, P., Marty, B., Hilton, D. R., Füri, E., Palhol, F., Sharp, Z. D., and Mangasini, F. (2009). Upper-mantle volatile chemistry at Oldoinyo Lengai volcano and the origin of carbonatites. *Nature*, 459, 77–80.

Freestone, I. C. and Hamilton, D. L. (1980). The role of liquid immiscibility in the genesis of carbonatites—An experimental study. *Contrib. Mineral. Petrol.*, 73, 105–117.

Guzmics, T., Mitchell, R. H., Szabó, C., Berkesi, M., Milke, R., and Ratter, K. (2012). Liquid immiscibility between silicate, carbonate and sulfide melts in melt inclusions hosted in co-precipitated minerals from Kerimasi volcano (Tanzania): evolution of carbonated nephelinitic magma. *Contrib. Mineral. Petrol.*, 164, 101–122.

Guzmics, T., Zajacz, Z., Mitchell, R. H., Szabó, C. S., and Wälle, M. (2015). The role of liquid–liquid immiscibility and crystal fractionation in the genesis of carbonatite magmas: insights from Kerimasi melt inclusions. *Contrib. Mineral. Petrol.*, 169, article no. 17.

Hamilton, D. L., Bedson, P., and Esson, J. (1989). The behaviour of trace elements in the evolution of carbonatites. In Bell, K., editor, *Carbonatites: Genesis and Evolution*, pages 405–427. Unwin Hyman, London.

Hammouda, T., Chantel, J., Manthilake, G., Guignard, J., and Crichton, W. (2014). Hot mantle geotherms stabilize calcic carbonate magmas up to the surface. *Geology*, 42(10), 911–914.

Hay, R. L. (1983). Natrocarbonatite tephra of Kerimasi volcano, Tanzania. *Geology*, 11, 599–602.

Jones, J. H., Walker, D., Pickett, D. A., Murrell, M. T., and Beattie, P. (1995). Experimental investigations of the partitioning of Nb, Mo, Ba, Ce, Pb, Ra, Th, Pa, and U between immiscible carbonate and silicate liquids. *Geochim. Cosmochim. Acta*, 59(7), 1307–1320.

Keller, J., Klaudius, J., Kervyn, M., Ernst, G. G. J., and Mattsson, H. B. (2010). Fundamental changes in the activity of the natrocarbonatite volcano Oldoinyo Lengai, Tanzania. I. New magma composition. *Bull. Volcanol.*, 72, 893–912.

Keller, J. and Krafft, M. (1990). Effusive natrocarbonatite activity at Oldoinyo Lengai, June 1988. *Bull. Volcanol.*, 52, 629–645.

Keller, J. and Zaitsev, A. N. (2006). Calciocarbonatitic dykes at Oldoinyo Lengai, Tanzania: the fate of natrocarbonatite. *Can. Mineral.*, 44, 857–876.

Keller, J. and Zaitsev, A. N. (2012). Reprint of "Geochemistry and petrogenetic significance of natrocarbonatites at Oldoinyo Lengai, Tanzania: Composition of lavas from 1988 to 2007". *Lithos*, 148, 45–53.

Kervyn, M., Ernst, G. G. J., Keller, J., Vaughan, G., Klaudius, J., Pradal, E., Belton, F., Mattsson, H., Mbede, E., and Jacobs, P. (2010). Fundamental changes in the activity of the natrocarbonatite volcano Oldoinyo Lengai, Tanzania. II. Eruptive behaviour. *Bull. Volcanol.*, 72, 913–931.

Kervyn, M., Klaudius, J., Keller, J., Mbede, E., Jacobs, P., and Ernst, G. G. J. (2008). Remote sensing study of sector collapses and debris avalanche deposits at Oldoinyo Lengai and Kerimasi volcanoes, Tanzania. *Int. J. Rem. Sens.*, 29, 6565–6595.

Kjarsgaard, B. and Peterson, T. (1991). Nephelinite–carbonatite liquid immiscibility at Shombole volcano, East Africa: petrographic and experimental evidence. *Mineral. Petrol.*, 43(4), 293–314.

Kjarsgaard, B. A. (1998). Phase relations of a carbonated high-CaO nephelinite at 0.2 and 0.5 GPa. *J. Petrol.*, 39(11–12), 2061–2075.

Kjarsgaard, B. A., Hamilton, D. L., and Peterson, T. D. (1995). Peralkaline nephelinite/carbonatite liquid immiscibility: Comparison of phase compositions in experiments and natural lavas from Oldoinyo Lengai. In Bell, K. and Keller, J., editors, *Carbonatite Volcanism. IAVCEI Proceedings in Volcanology*, volume 4, pages 163–190. Springer, Berlin, Heidelberg.

Klaudius, J. and Keller, J. (2006). Peralkaline silicate lavas at Oldoinyo Lengai, Tanzania. *Lithos*, 91, 173–190.

Kogarko, L. N., Plant, D. A., Henderson, C. M. B., and Kjarsgaard, B. A. (1991). Na-rich carbonate inclusions in perovskite and calzirtite from the Guli intrusive Ca-carbonatite, polar Siberia. *Contrib. Mineral. Petrol.*, 109(1), 124–129.

Le Bas, M. J., Mills, A. A., and Rankin, A. H. (1972). Preliminary evidence on the nature and composition of carbonatite magma. *Nature*, 239, 215.

Le Maitre, R. W., Bateman, P., Dudek, A., Keller, J., Lameyre, J., Le Bas, M. J., Sabine, P. A., Schmid, R., Sorensen, H., Streckeisen, A., Woolley, A. R., and Zanettin, B. (1989). *A Classification of Igneous Rocks and Glossary of Terms*. Blackwell Scientific Oxford Bibliografía. pages 130–171.

Ling, M. X., Liu, Y. L., Williams, I. S., Teng, F. Z., Yang, X. Y., Ding, X., Wei, G. J., Xie, L. H., Deng, W. F., and Sun, W. D. (2013). Formation of the world's largest REE deposit through protracted fluxing of carbonatite by subduction-derived fluids. *Sci. Rep.*, 3, article no. 1776.

Martin, L. H. J., Schmidt, M. W., Mattsson, H. B., and Guenther, D. (2013). Element partitioning between immiscible carbonatite and silicate melts for dry and H_2O-bearing systems at 1–3 GPa. *J. Petrol.*, 54(11), 2301–2338.

Masotta, M., Mollo, S., Freda, C., Gaeta, M., and Moore, G. (2013). Clinopyroxene–liquid thermometers and barometers specific to alkaline differentiated magmas. *Contrib. Mineral. Petrol.*, 166(6), 1545–1561.

Mitchell, R. H. (2009). Peralkaline nephelinite–natrocarbonatite immiscibility and carbonatite assimilation at Oldoinyo Lengai, Tanzania. *Contrib. Mineral. Petrol.*, 158, 589–598.

Mollex, G. (2017). *Architecture de la plomberie du volcan carbonatitique Oldoinyo Lengai: nouvelles contraintes sur la source, les transferts hydrothermaux, et la différenciation magmatique dans la chambre active*. PhD thesis, Université de Lorraine.

Mollex, G., Füri, E., Burnard, P., Zimmermann, L., Chazot, G., Kazimoto, E. O., Marty, B., and France, L. (2018). Tracing helium isotope compositions from mantle source to fumaroles at Oldoinyo Lengai volcano, Tanzania. *Chem. Geol.*, 480, 66–74.

Nabyl, Z., Massuyeau, M., Gaillard, F., Tuduri, J., Iacono-Marziano, G., Rogerie, G., Le Trong, E., Di Carlo, I., Melleton, J., and Bailly, L. (2020). A window in the course of alkaline magma differentiation conducive to immiscible REE-rich carbonatites. *Geochim. Cosmochim. Acta*, 282, 297–323.

Peterson, T. D. (1989). Peralkaline nephelinites II. Low pressure fractionation and the hypersodic lavas of Oldoinyo L'engai. *Contrib. Mineral. Petrol.*, 102, 336–346.

Pouchou, J. L. and Pichoir, F. (1991). Quantitative analysis of homogeneous or stratified microvolumes applying the model "PAP". In Heinrich, K. F. J. and Newbury, D. E., editors, *Electron Probe Quantification*, pages 31–75. Plenum, New York.

Rose-Koga, E., Bouvier, A.-S., Gaetani, G., Wallace, P. J., Allison, C. M., Andrys, J. A., et al. (2021). Silicate melt inclusions in the new millennium: a review of recommended practices for preparation, analysis, and data presentation. *Chem. Geol.*, 570, article no. 120145.

Schmidt, M. W. and Weidendorfer, D. (2018). Carbonatites in oceanic hotspots. *Geology*, 46, 435–438.

Sharygin, V. V., Kamenetsky, V. S., Zaitsev, A. N., and Kamenetsky, M. B. (2012). Silicate–natrocarbonatite liquid immiscibility in 1917 eruption combeite–wollastonite nephelinite Oldoinyo Lengai Volcano Tanzania: melt inclusion study. *Lithos*, 152, 23–39.

Sherrod, D. R., Magigita, M. M., and Kwelwa, S. (2013). Geologic map of Oldonyo Lengai (Oldoinyo Lengai) and surroundings, Arusha Region, United Republic of Tanzania. U. S. Geological Survey Open-File Report No. 2013-1306.

Uhlig, C. (1905). Bericht über die Expedition der Otto-Winter-Stiftung nach den Umgebungen des Meru. *Zeitschrift der Gesellschaft für Erdkunde zu Berlin*, 1905, 120–123.

Veksler, I. V., Dorfman, A. M., Dulski, P., Kamenetsky, V. S., Danyushevsky, L. V., Jeffries, T., and Dingwell, D. B. (2012). Partitioning of elements between silicate melt and immiscible fluoride, chloride, carbonate, phosphate and sulfate melts, with implications to the origin of natrocarbonatite. *Geochim. Cosmochim. Acta*, 79, 20–40.

Veksler, I. V., Petibon, C., Jenner, G. A., Dorfman, A. M., and Dingwell, D. B. (1998). Trace element partitioning in immiscible silicate–carbonate liquid systems: an initial ex- perimental study using a centrifuge autoclave. *J. Petrol.*, 39(11–12), 2095–2104.

Verplanck, P. L., Van Gosen, B. S., Seal, R. R., and McCafferty, A. E. (2014). A deposit model for carbonatite and peralkaline intrusion-related rare earth element deposits. In *Mineral Deposit Models for Resource Assessment*, page 58. U.S. Geological Survey.

Weidendorfer, D., Schmidt, M. W., and Mattsson, H. B. (2016). Fractional crystallization of Si-undersaturated alkaline magmas leading to un-

mixing of carbonatites on Brava Island (Cape Verde) and a general model of carbonatite genesis in alkaline magma suites. *Contrib. Mineral. Petrol.*, 171, article no. 43.

Weidendorfer, D., Schmidt, M. W., and Mattsson, H. B. (2017). A common origin of carbonatite magmas. *Geology*, 45(6), 507–510.

Woolley, A. R. and Kjarsgaard, B. A. (2008). *Carbonatite occurrences of the world: map and database*. Natural Resources Canada. Geological Survey of Canada, Open File 5796, 28 pages (1 sheet).

Zaitsev, A. N. and Keller, J. (2006). Mineralogical and chemical transformation of Oldoinyo Lengai natrocarbonatites, Tanzania. *Lithos*, 91, 191–207.